Fig S1

A

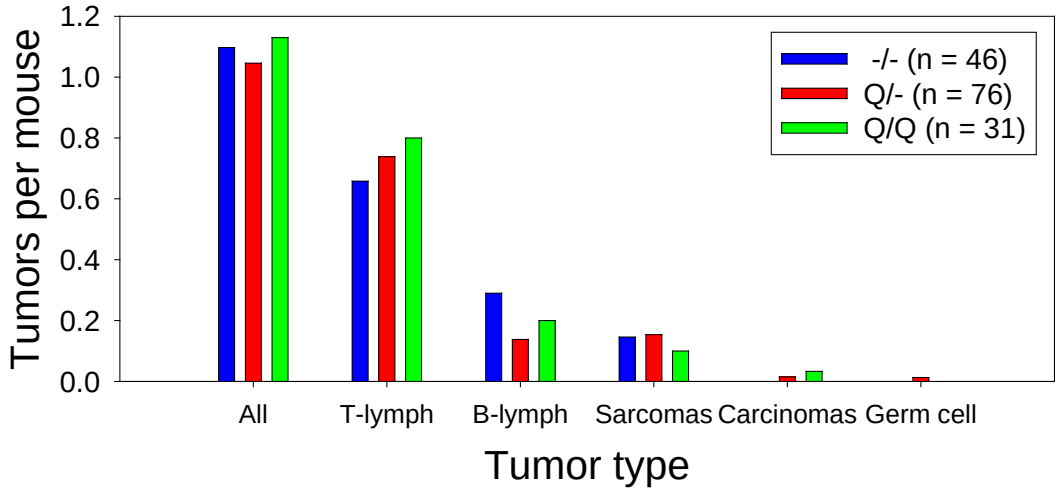

B

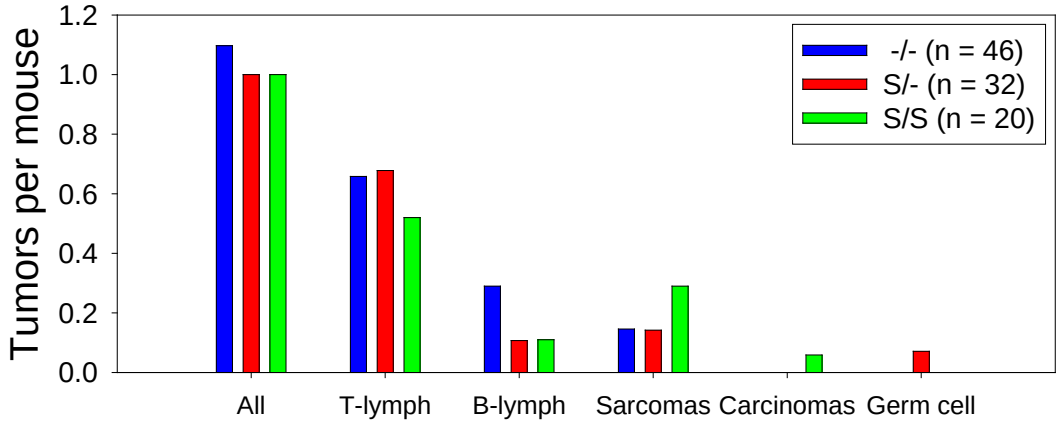

Fig. S1. R248Q and G245S alleles display a modest broadening of tumor spectrum compared to p53 null allele.
Tumors per mouse of the indicated tumor subtypes. The y-axis indicates the total number of tumors within a category (e.g. T-lymph) divided by the total number of mice within the indicated genotype. **A,** null, R248Q/- and R248Q/R248Q mice. **B,** null, G245S/- and G245S/G245S mice.

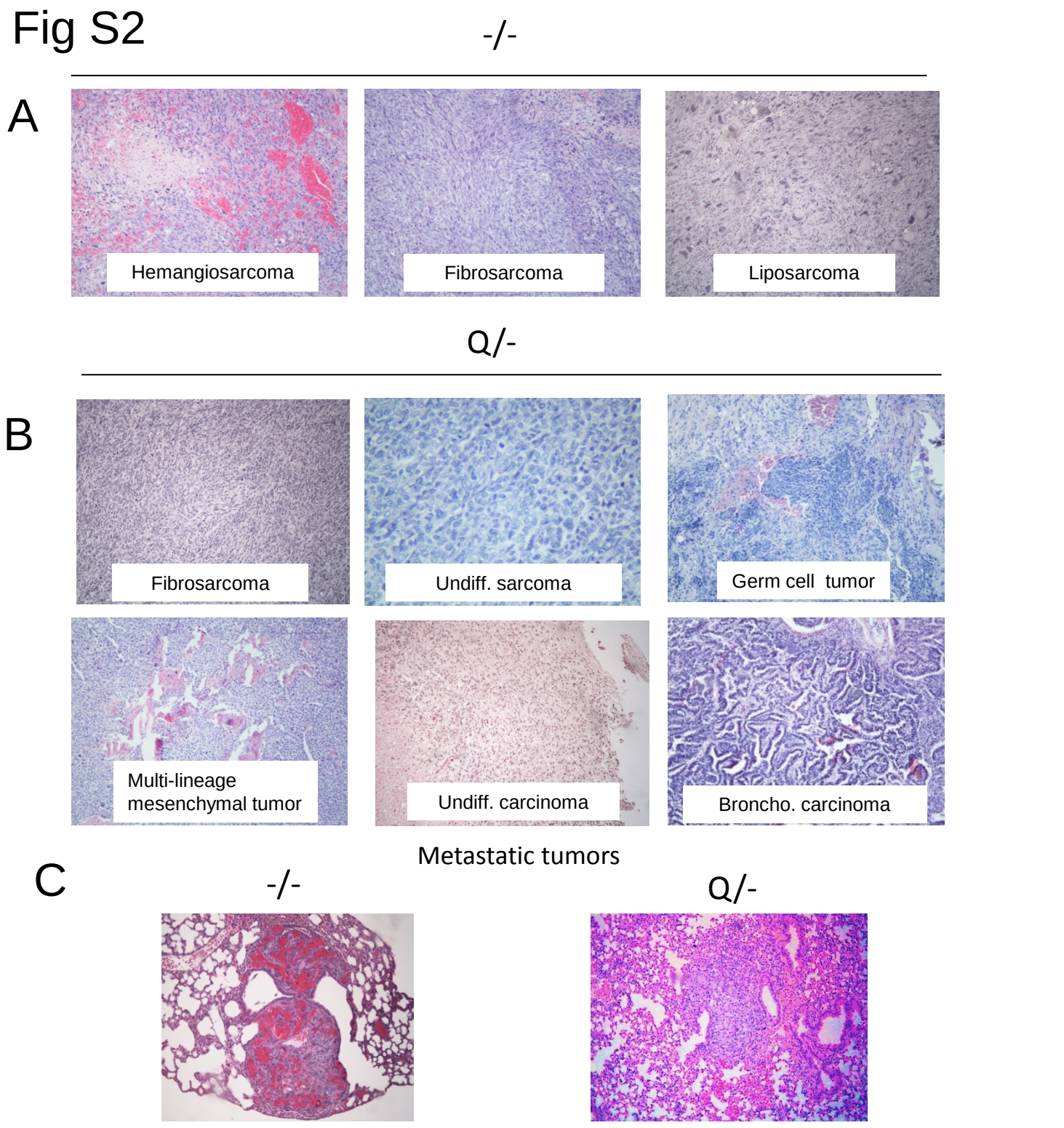

Fig. S2. Expression of R248Q results in a broader histological spectrum of tumor types. Similar results were seen in G245S mice.

A. p53-null mice developed hemangiosarcoma, fibrosarcoma and rarely liposarcoma.

B. Examples of p53R248Q/- mice developing fibrosarcoma, undifferentiated sarcoma, abdominal germ cell tumor, multi-lineage mesenchymal tumor with areas of osteoid and pericyte differentiation, undifferentiated carcinoma with areas of
glandular differentiation, and bronchoalveolar carcinoma of the lung.

C. *Left* one p53 null mouse developed a large diffuse hemangiosarcoma of the heart that had seeded multiple tumor emboli to the lung. *Right* one R248Q/- mouse developed a large fibrosarcoma in the abdomen that generated multiple distant metastases into the lungs and numerous subcutaneous nodules on the back.

Table S1

Table S1. Histological types of all solid tumors that arose in the indicated genotypes.

-/-	Q/-	Q/Q	S/-	S/S
Hemangiosarcoma (3/6) Fibrosarcoma (2/6) Liposarcoma (1/6)	Fibrosarcoma (3/12) Hemangiosarcoma (2/12) Undiff. Sarcoma (2/12) Germ Cell tumor (1/12) Mutlilineage mesenchym. tumor (1/12) Lung carcinoma (1/12) Undiff. Carcinoma (1/12)	Fibrosarcoma (3/4) Undiff.carcinoma (1/4)	Fibrosarcoma (2/6) Hemangiosarcoma (1/6) Germ cell tumor (2/6) Undiff. Carcinoma (1/6)	Fibrosarcoma (3/6) Undiff. Sarcoma (1/6) Hemangiosarcoma (1/6) Eccrine carcinoma (1/6)

In parenthesis are the number of tumors per total number of solid tumors of the indicated genotypes.

Fig S3

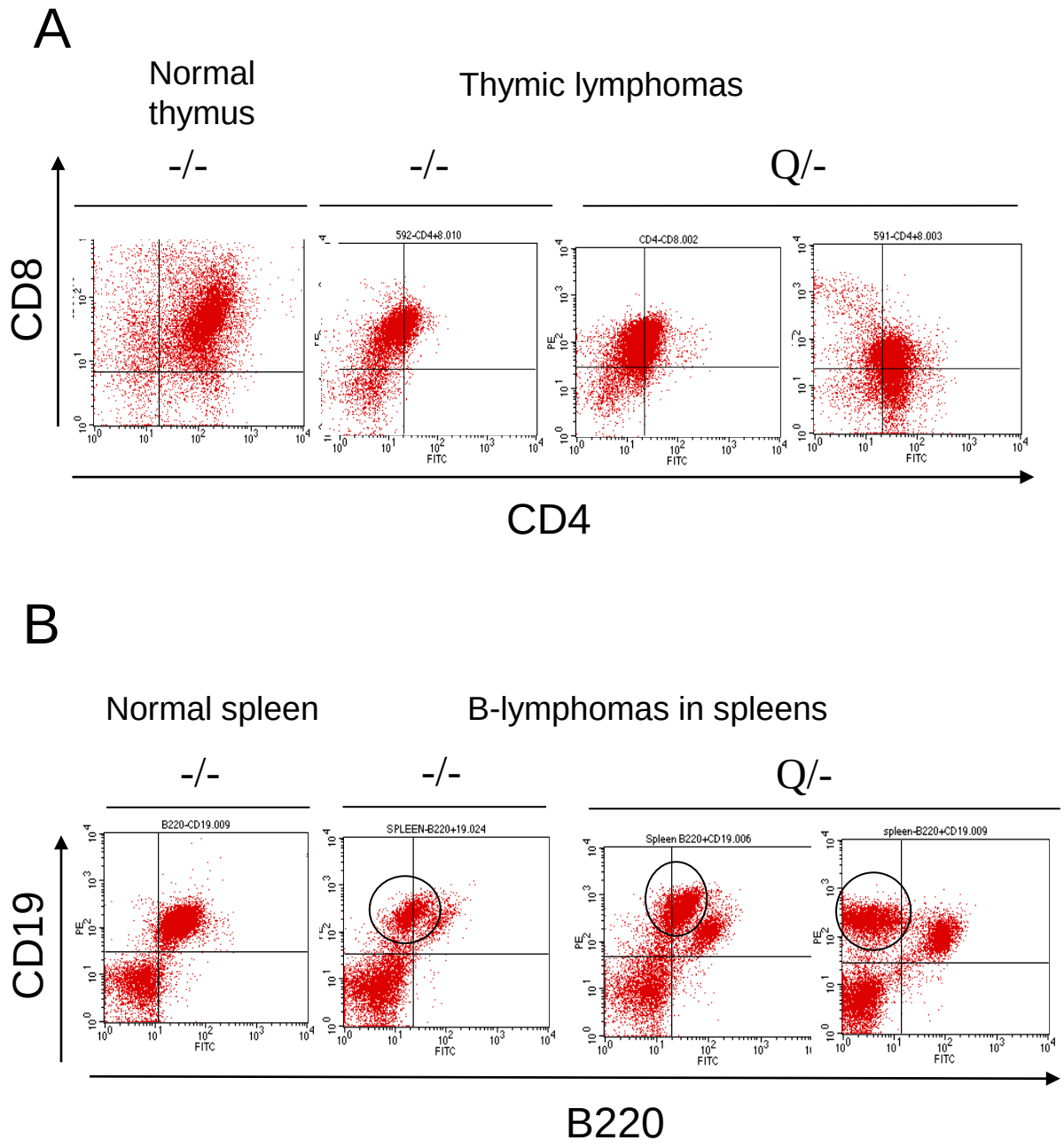

Fig. S3. p53 -/- and R248Q/- T and B-cell lymphomas display similar surface phenotypes

A. *Left,* Normal thymus and *Right* T-lymphomas from p53 -/- and R248Q/- mice,
B. *Left,* Normal spleen and *Right* B-lymphomas from p53 -/- and R248Q/- mice, with leukemic populations circled. FACS analysis.

Fig S4

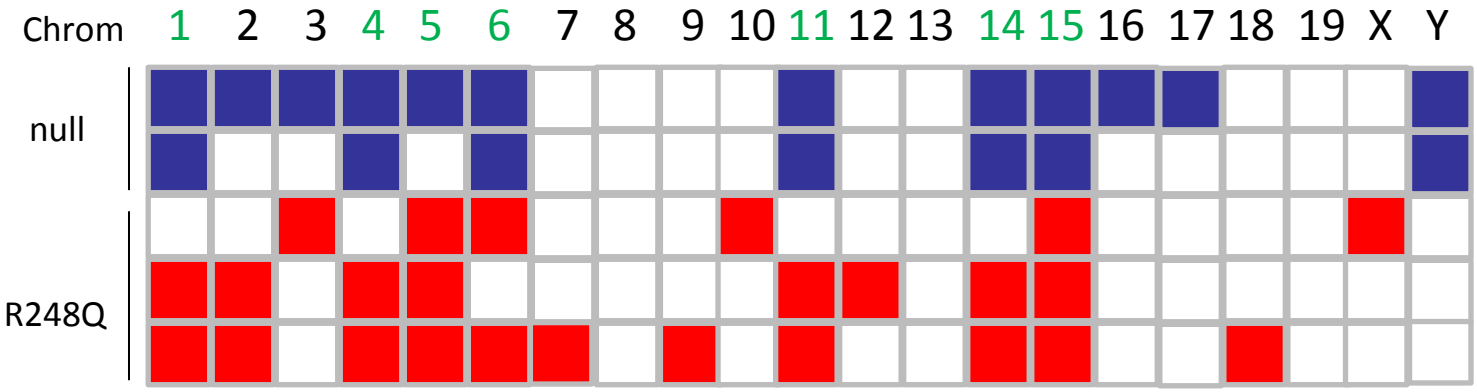

Chromosomal structural abnormalities

-/-	Q/-	Q/Q
(Y;1)- (11/20) Deletion(del16) (11/20) t(2;X)- (18/20) t(14;X)- (20/20)	del(3)-(25/30) der(3)t(3;19)-(13/30) t(4;16)-(17/20)	(9:12)- (14/20)

Fig. S4. Both R248Q and p53 null T-lymphomas display extensive aneuploidy and contain clonal translocations.
Top Chromosome ID displaying numerical aneuploidy in >50% of metaphases analyzed from two p53 null cell lines (blue) and three R248Q cell lines (red). Chromosomes in green are aneuploid in at least four of the five cell lines analyzed. *Bottom* Specific clonal translocations found within the cell lines analyzed. In parenthesis is the number of metaphases displaying the translocation over total number of metaphases analyzed for that cell line.

Fig S5

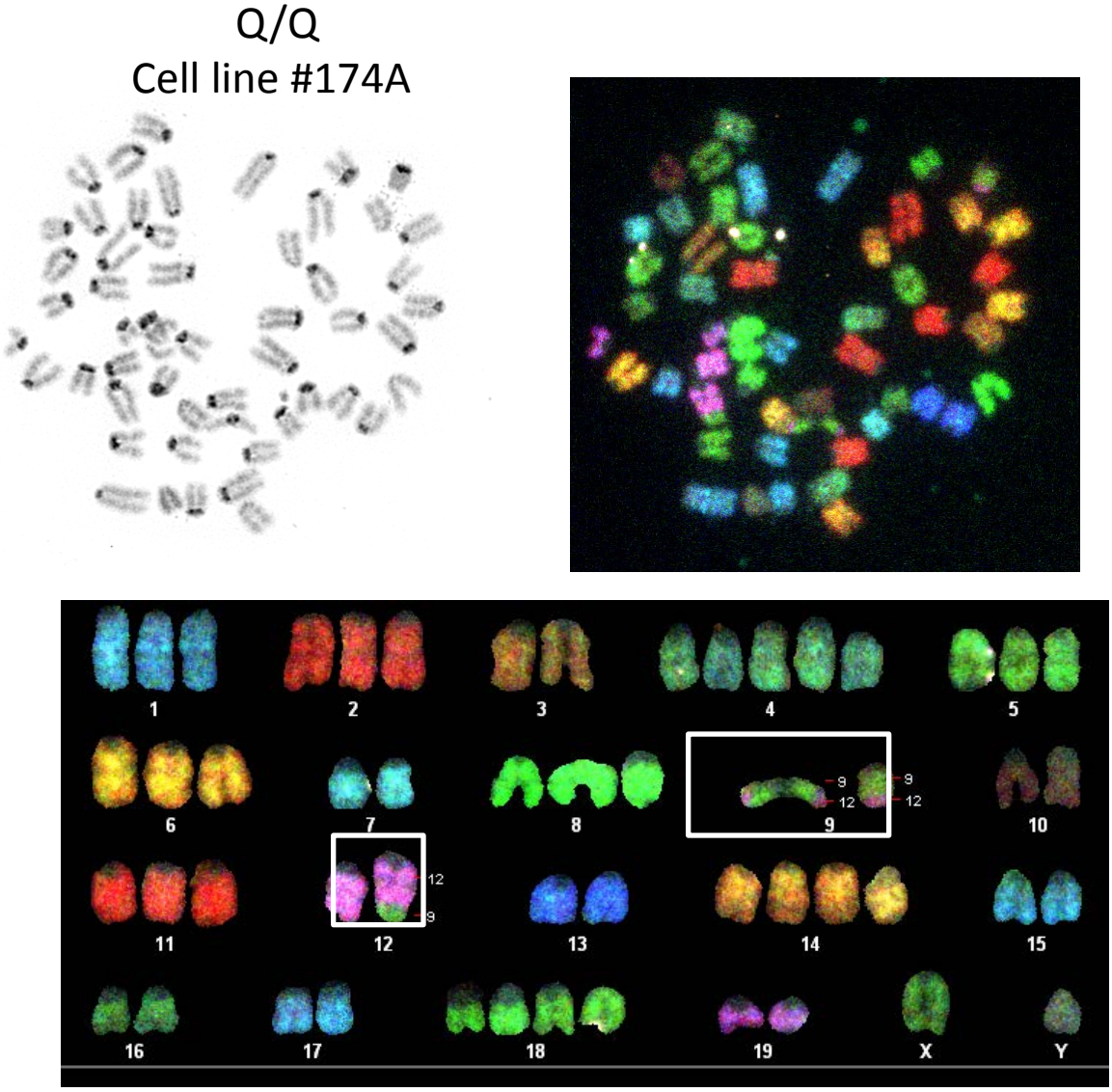

Fig. S5. R248Q/Q T-lymphoma displays extensive aneuploidy and contains clonal translocations. Metaphases from a homozygous R248Q/R248Q cell line at early passage exhibits extensive aneuploidy and a 9:12 translocation (boxed). *Upper left* Giemsa staining, *upper right* and *bottom* SKY analysis.

Fig S6

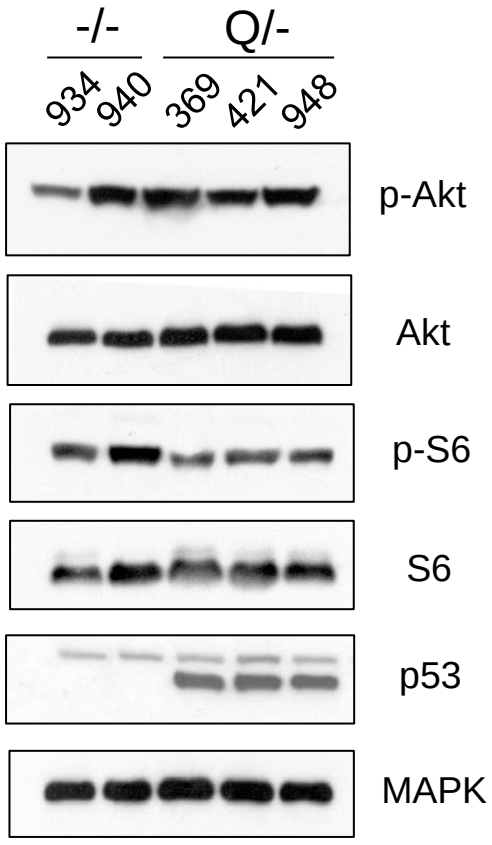

Fig. S6. In culture T-lymphoma cell lines derived from -/- and Q/- mice display similar signaling through the Akt pathway.
Protein lysates from T-lymphoma cell lines in tissue culture from -/- and Q/- mice were blotted for p-Akt, total Akt, p-S6, total S-6, and MAPK.

Fig S7

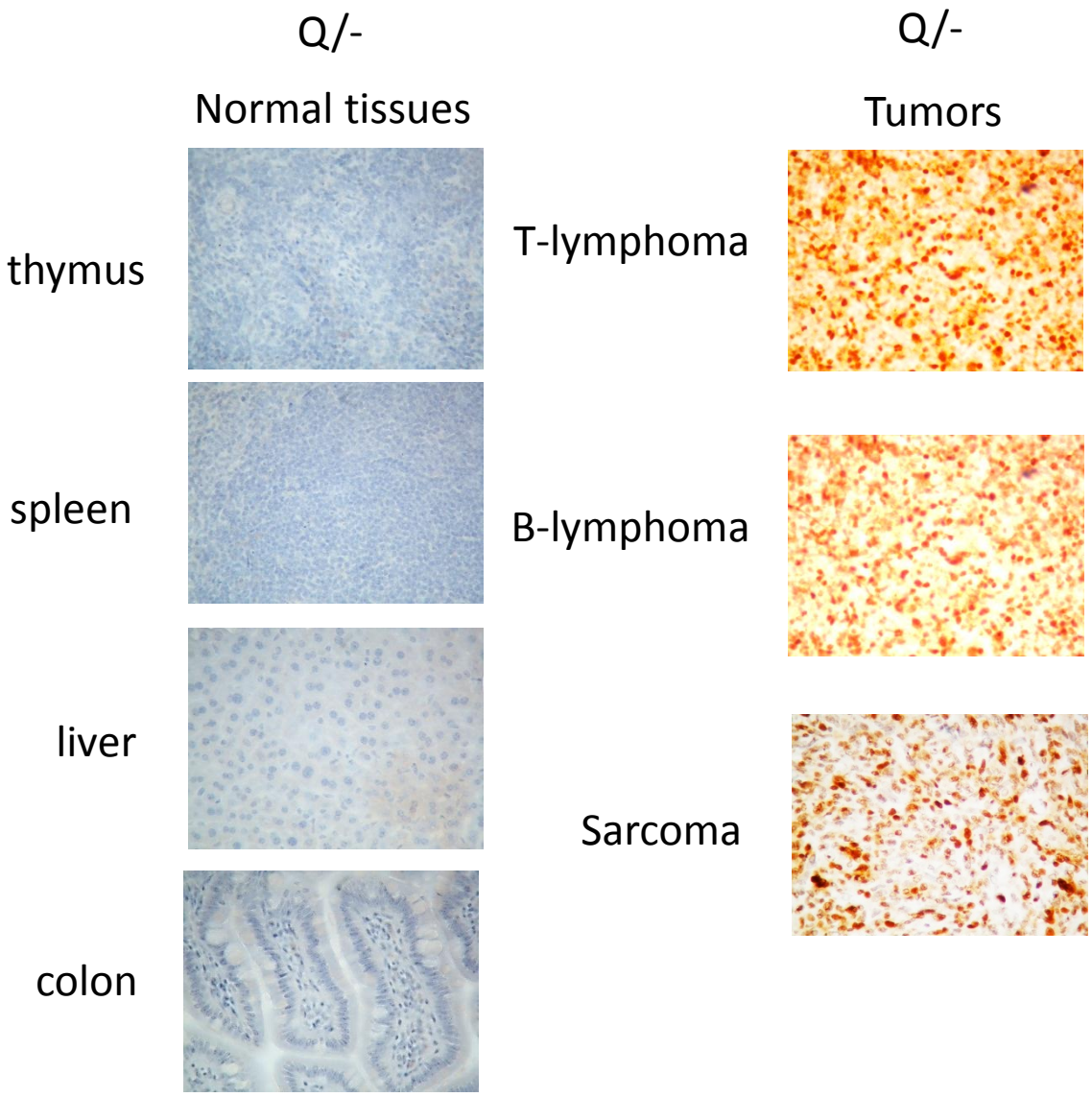

Fig. S7. mutp53 R248Q protein becomes stabilized only in tumor tissues but not in normal tissues.
Normal tissues *left* and different tumors *right* from R248Q/- mice were stained side by side for the presence of detectable p53 protein (brown) and counterstained by hematoxylin (blue).

Fig S8

A

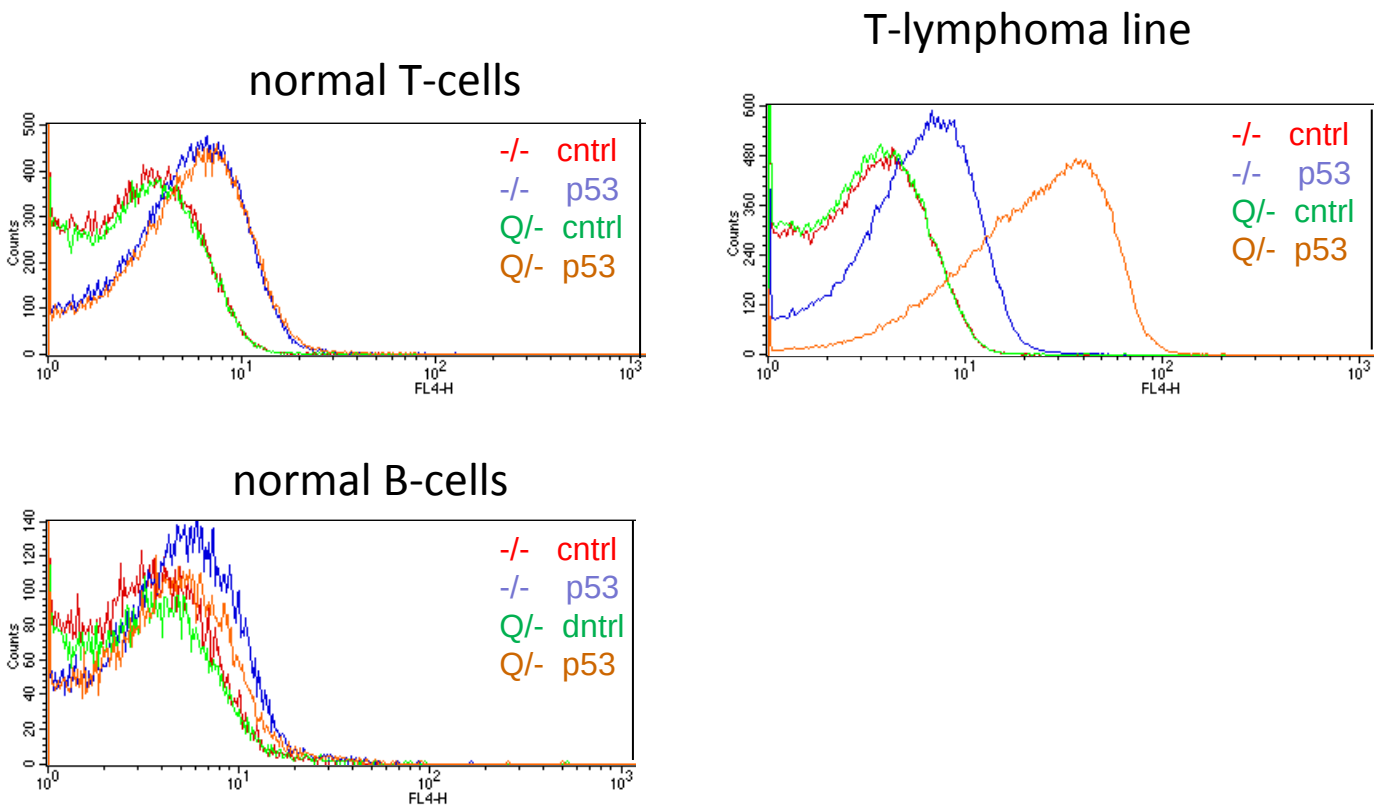

B

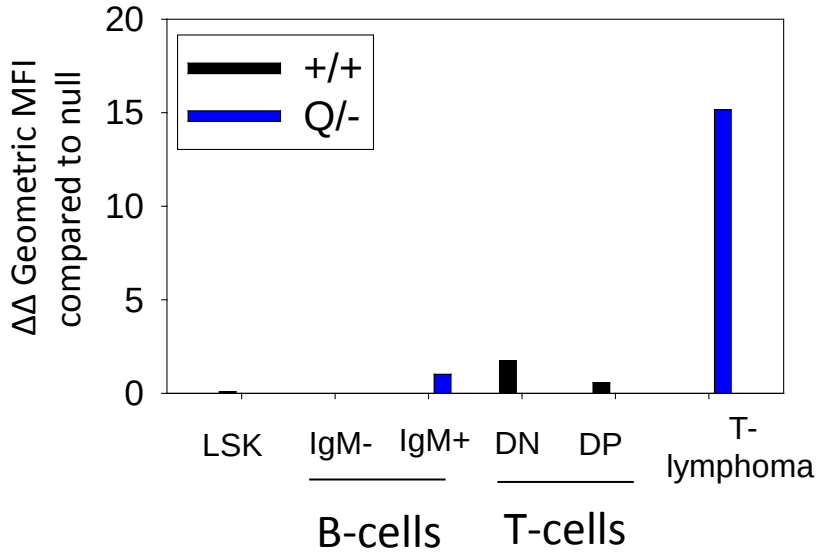

Fig. S8. mutp53 R248Q protein becomes stabilized only in tumor tissues but not in normal tissues.

A. Histograms of normal B-lymphocytes, T-lymphocytes and malignant T- lymphoma cells of the indicated genotypes with and without intracellular staining for p53. FACS analysis.

B. Quantification of changes in geometric mean fluorescence intensity (MFI) measured in panel A for individual cell populations after correction for background staining in p53 -/- cells.

Fig S9

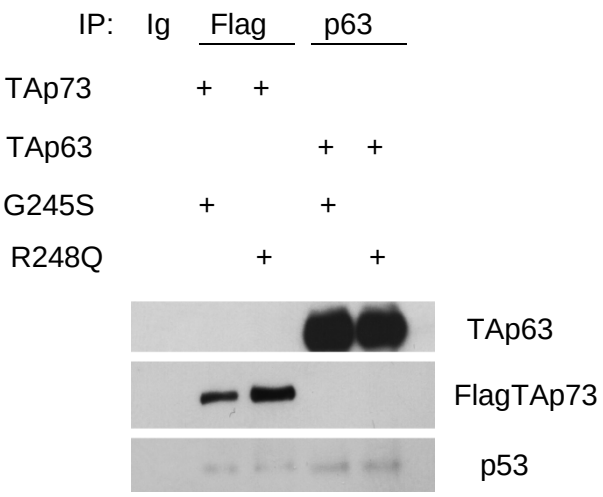

Fig. S9. mutp53 R248Q and G245S do not differ in their binding to TAp63 and TAp73.
HCT116 p53-/- cells were transfected with FlagTAp73 + G245S and R248Q or TAp63 + G245S and R248Q, respectively. Twenty-four hours post transfected cells were harvested and immunoprecipitated followed by immunoblotting as indicated.

Fig S10

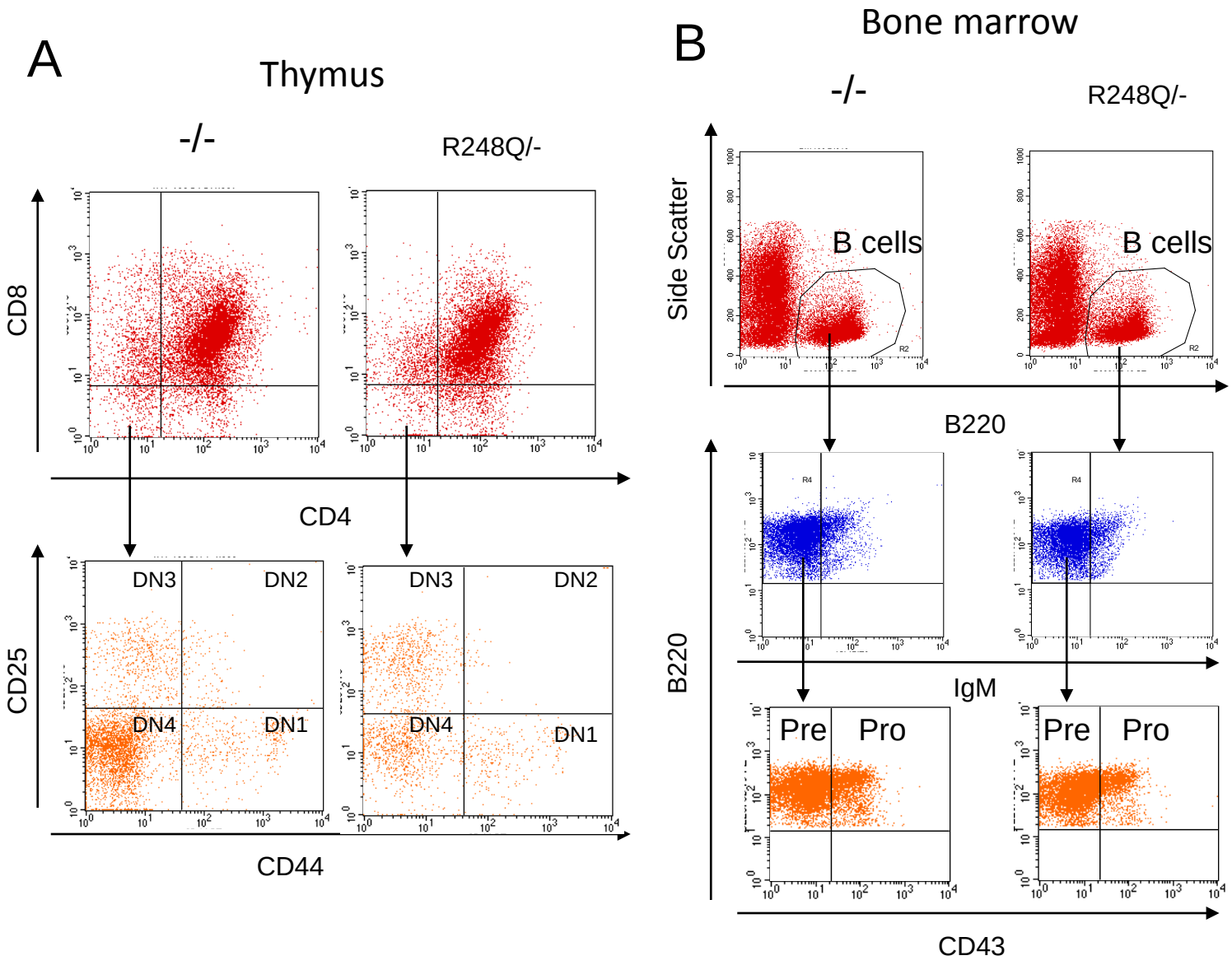

Fig. S10. Gating strategy for evaluating the differentiation of subpopulations of T and B lymphocytes.
A. *Top* DP, CD8, CD4 and DN subpopulations from 4-5 week old thymi of p53 -/- and R248Q/- mice. *Bottom* DN1 (CD44+CD25-), DN2 (CD44+CD25+), DN3 (CD44-CD25+), and DN4 (CD44-CD25-) subpopulations from the DN (CD8-CD4-) subset of p53 -/- and R248Q/- mice.
B. B-cell populations from bone marrow of 4-5 week old p53 -/- and R248Q/- mice, gating for *top* total B-cells (side scatter and B220+), *middle* mature (B220+IgM+) and immature (B220+IgM-) B-cells, and *bottom* pro (B220+IgM-CD43+) and pre (B220+IgM-CD43-) B-cells.

Fig S11

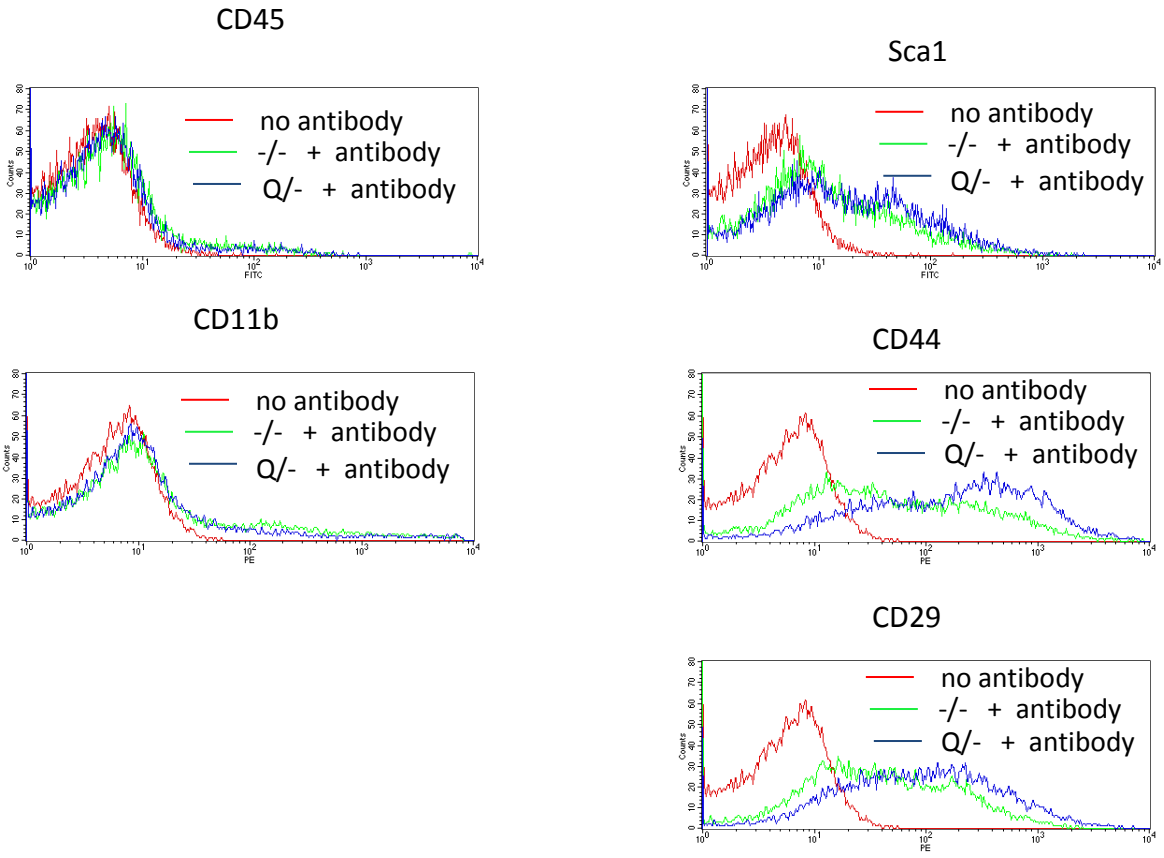

Fig. S11. Mesenchymal stem cells derived from p53-/- and R248Q/- mice express MSC markers and lack hematopoeitic markers.
Adherent fibroblast colonies from the bone marrow of -/- and Q/- mice were probed for *left* expression of CD45 and CD11b (hematopoetic markers) and *right* expression of Sca1, CD44 and CD29 (MSC markers).

.

Fig S12

p21
5’-CCTGGTGATGTCCGACCTG-3’
5’-CGGGACCGAAGAGACAACG-3’

PUMA
5’-AGCAGCACTTAGAGTCGCC-3’
5’-CCTGGGTAAGGGGAGGAGT-3’

HPRT
5'-GGGGGCTATAAGTTCTTTGC-3'
5'-TCCAACACTTCGAGAGGTCC-3'

Fig. S12. Primers used in real-time qRT-PCR experiments for the indicated genes.

Fig S13

Thymocyte stain	Cell populations
1. CD4-PE CD8-FITC TER119-APC CD19-APC Mac1-APC	**DP** APC- PE + FITC + **DN** APC- PE + FITC -
2. CD4-APC CD8-APC TER119-APC CD19-APC Mac-1-APC CD25-FITC CD44-PE	**DN1** APC- PE+ FITC- **DN2** APC- PE+ FITC+ **DN3** APC- PE- FITC+ **DN4** APC- PE- FITC-

Bone marrow stain	Cell populations
1. CD19-PE B220-PE Mac1-PE Gr1-PE ckit-APC Sca1-FITC	**LSK** PE- APC + FITC +
2. B220-PE CD19-PE CD43-APC IgM-FITC	**Total B-cells** PE+ **Pro** PE+ APC+ **Pre** PE+ APC- **Immature** PE+ FITC+ **Mature** PE+ FITC-

Spleen stain	Cell population
1. B220-PE CD19-PE CD43-APC IgM-FITC	**Total B-cells** PE+ **Pro** PE+ APC+ **Pre** PE+ APC- **Immature** PE+ FITC+ **Mature** PE+ FITC-
2. IgM-FITC IgD- PE	**IgM + IgD +** FITC + PE +

p53 staining

Thymocyte stain	Cell populations
1. CD4-PE CD8-FITC p53-AlexaR647	**DP** PE+ FITC+ **DN** PE- FITC-

Bone marrow stain	Cell populations
1. B220-PE Mac1-PE Gr1-PE CD3-PE TER119-PE ckit-PerCP-eFluor710 Sca1-FITC p53-AlexaR647	**LSK** PE- PerCP+ FITC +
2. B220-PE IgM-FITC p53-AlexaR647	**Total B-cells** PE+ **Immature** PE+ FITC- **Mature** PE+ FITC+

Fig. S13. Antibodies used and gating strategies for indicated subpopulations in lymphocyte development experiments (Fig. 8 and Fig. S9).